Supporting Information for "Predicting the three-dimensional age-depth field of an ice rise"

A. C. J. Henry[1,2,3], C. Schannwell[1], V. Višnjević[2], J. Millstein[4], P. D. Bons[2], O. Eisen[5,6], R. Drews[2]

[1]Max Planck Institute for Meteorology, Hamburg, Germany

[2]Department of Geosciences, University of Tübingen, Tübingen, Germany

[3]International Max Planck Research School on Earth System Modelling, Max Planck Institute for Meteorology, Hamburg, Germany

[4]Massachusetts Institute of Technology—Woods Hole Oceanographic Institute Joint Program in Oceanography/Applied Ocean Science and Engineering, Cambridge, MA, USA

[5]Alfred Wegener Institute Helmholtz Centre for Polar and Marine Research, Bremerhaven, Germany

[6]University of Bremen, Bremen, Germany

Contents of this file

1. Figures S1 to S10

Introduction

The supporting information contains additional figures pertaining to the simulations described in the main article. Figures included show (1) the age at 50 and 95 % depth for the simulations using Glen's flow law exponents of $n = 3$ and $n = 4$, (2) the percentage difference in velocity magnitude at the surface and at the 1000 year isochrone for the $n = 3$ and $n = 4$ simulations, (3) the basal velocity magnitude for the $n = 4$ simulation

and the difference in basal velocity magnitude between the $n = 3$ and $n = 4$ simulations, (4) the horizontal surface dilation for the $n = 3$ and $n = 4$ simulations and the difference between the two, (5) comparisons between RACMO2.3p1, stratigraphy-derived and drift-corrected surface mass balance (SMB) fields, (6) vertical temperature evolution profiles sampled at two coordinates, (7) comparisons between observed and modelled stratigraphy for all $n = 3$ and $n = 4$ simulation cross-sections not included in the main article and (8) the slope difference between the modelled and observed stratigraphy for the cross-section $G - G'$.

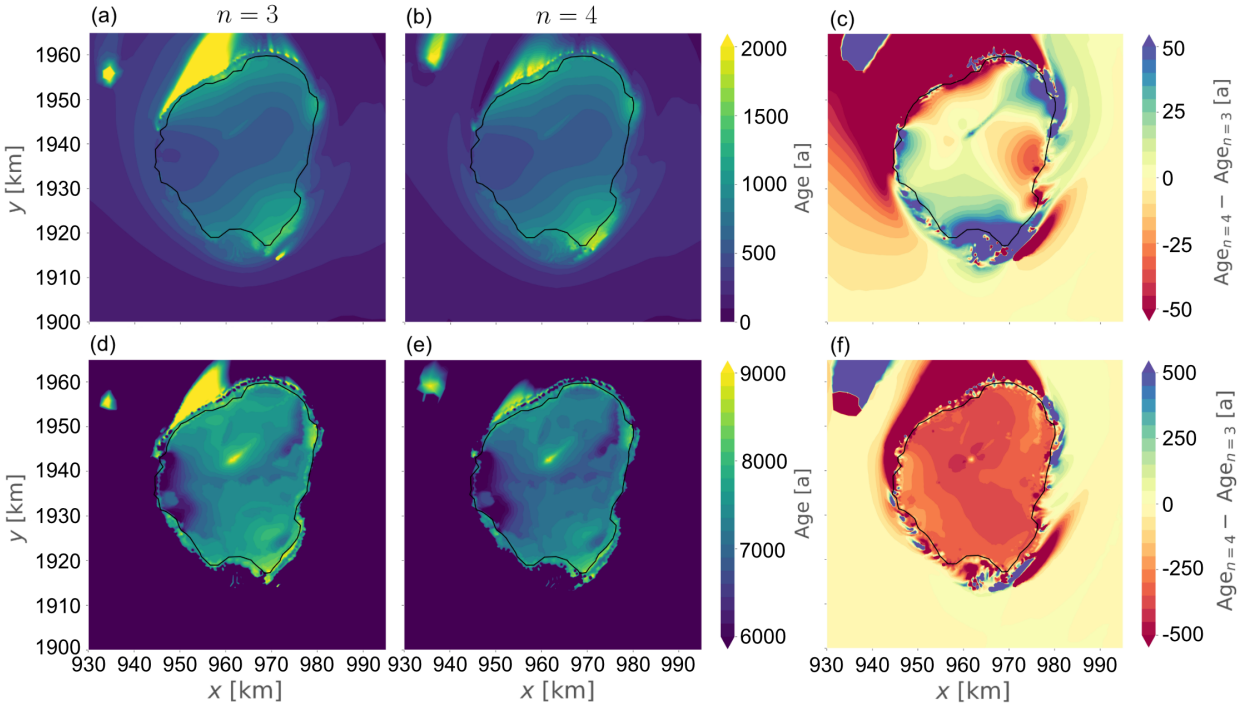

Figure S1. In (a) and (b), the age of the ice is shown at a depth of 50 % for the $n = 3$ and $n = 4$ simulations, respectively, and in (c), the difference between the $n = 4$ and the $n = 3$ simulations. In (d) and (e), the age of the ice is shown at a depth of 95 % for the $n = 3$ and $n = 4$ simulations, respectively. In (c) and (f), the difference between the age in the $n = 4$ and the $n = 3$ simulations is shown for a depth of 50 % and 95 %, respectively.

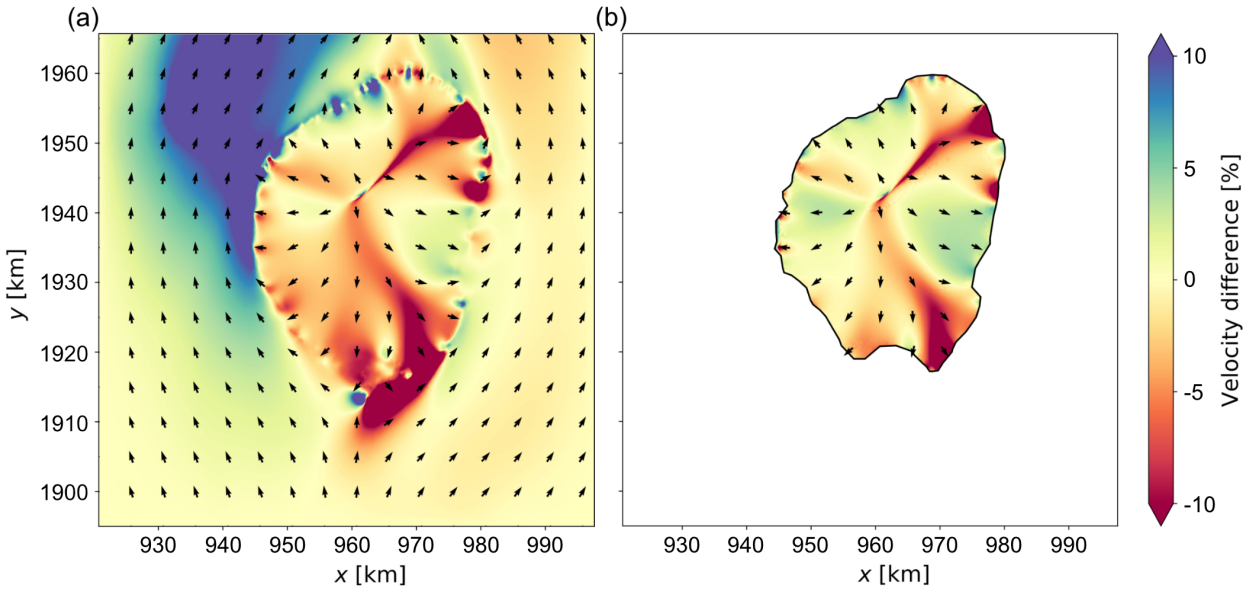

Figure S2. In (a), the percentage difference between the surface velocity magnitudes in the case of the $n = 4$ simulation and the $n = 3$ simulation. In (b), the percentage difference between the velocity magnitudes at the $Age = 1000$ a isochrone in the case of the $n = 4$ simulation and the $n = 3$ simulation. The arrows indicate the velocity directions of the $n = 3$ simulation. Note that the velocity magnitude of the $n = 3$ simulation is subtracted from the velocity magnitude of the $n = 4$ simulation.

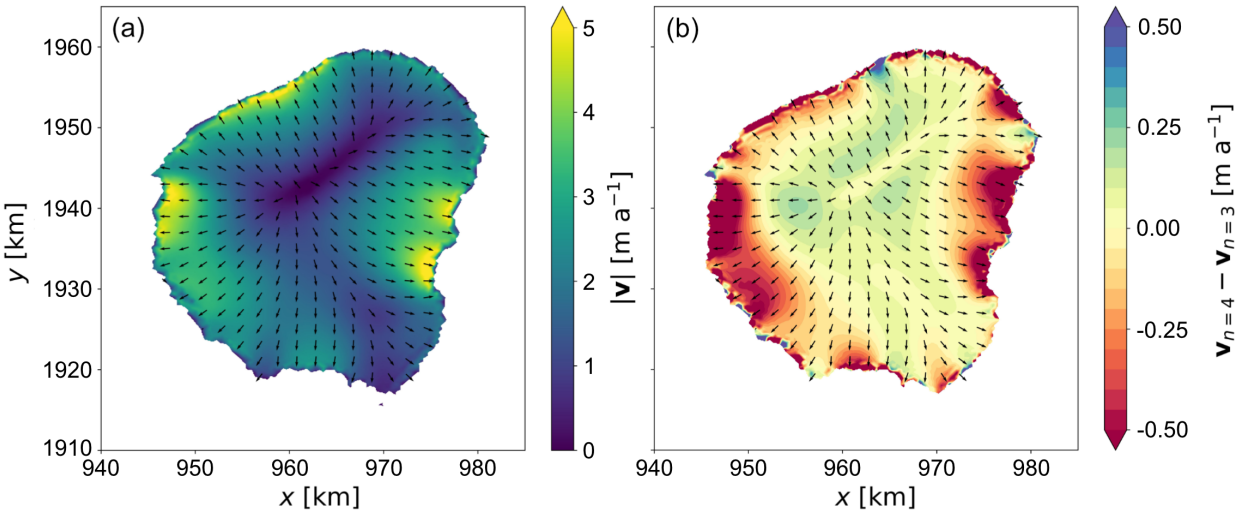

Figure S3. The basal velocity of the $n = 4$ simulation is shown in (a). The colour indicates the velocity magnitude and the arrows indicate the velocity direction. The basal velocity magnitude difference between the $n = 3$ and the $n = 4$ simulation is shown in (b). Note that the basal velocity magnitude of the $n = 3$ simulation is subtracted from the basal velocity magnitude of the $n = 4$ simulation.

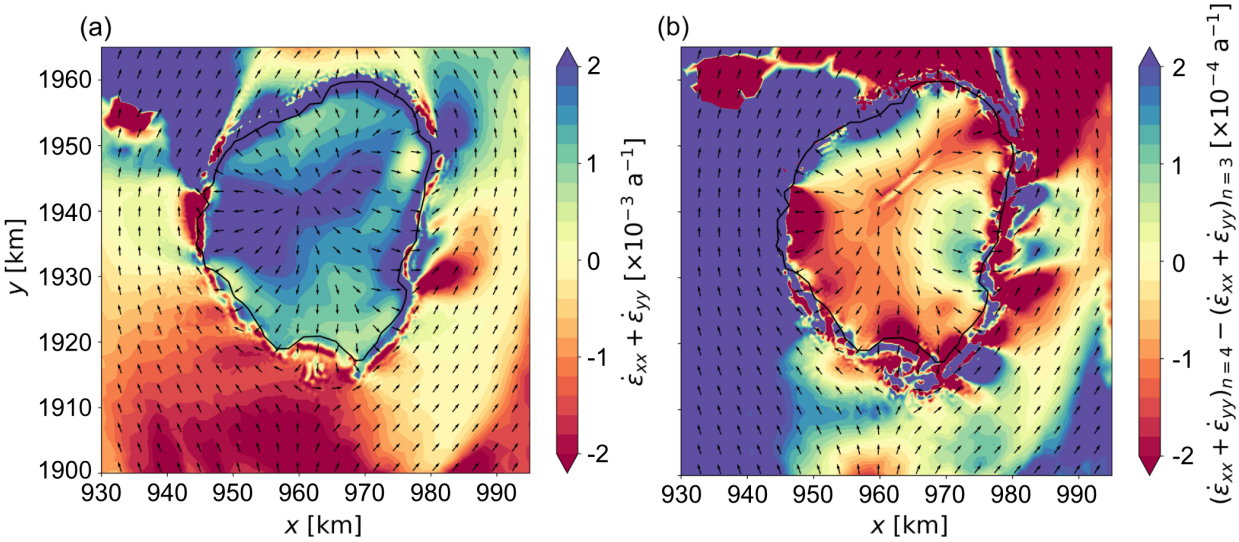

Figure S4. In (a), the horizontal dilation of the velocity field in the case of the $n = 3$ simulation is shown. In (b), the difference between the horizontal dilation in the case of the $n = 4$ and $n = 3$ simulations is shown. Note that the dilation of the $n = 3$ simulation is subtracted from the dilation of the $n = 4$ simulation.

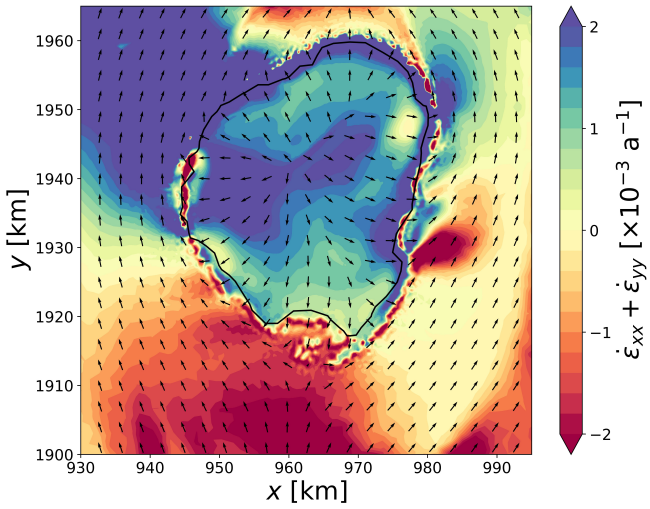

Figure S5. The horizontal dilation of the velocity field in the case of the $n = 4$ simulation.

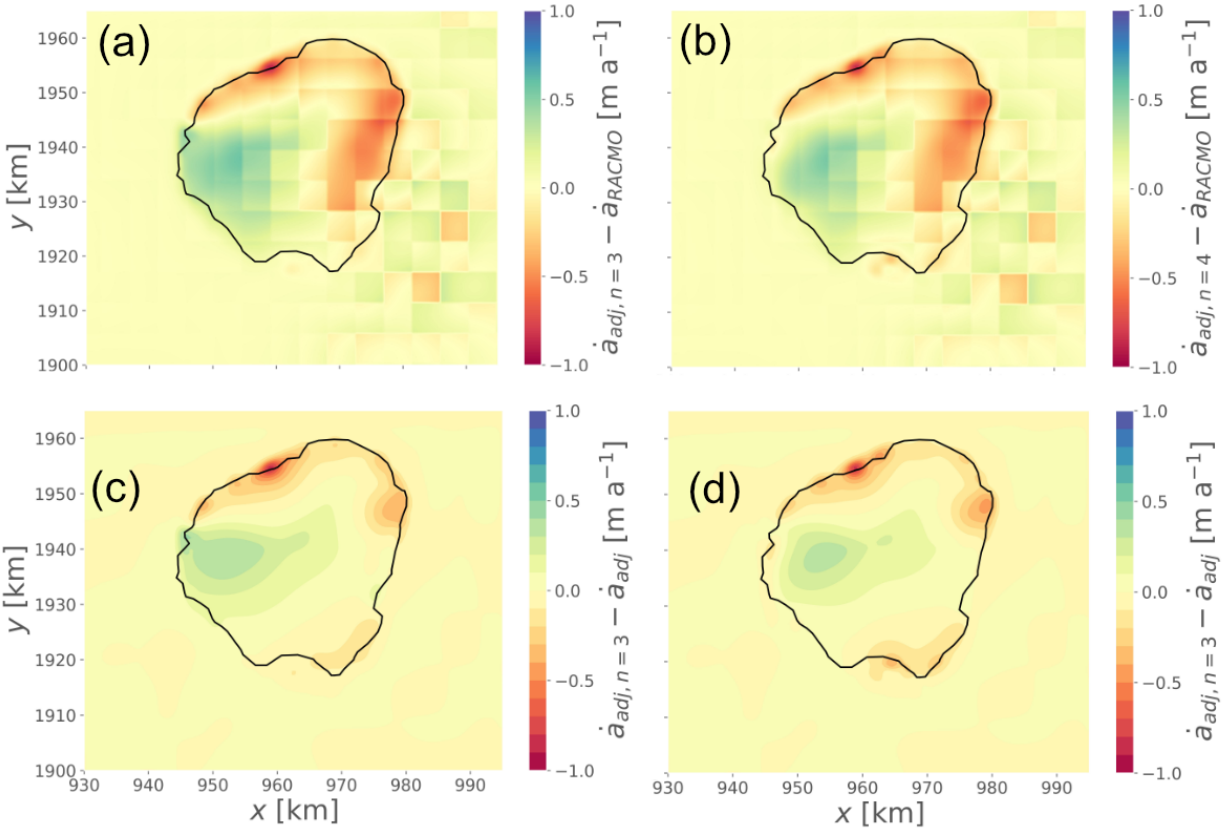

Figure S6. (a) and (b) show the difference between the SMB of the $n = 3$ and the RACMO2.3p1 data, and between the $n = 4$ simulations and the RACMO2.3p1 data , respectively. (c) and (d) show the difference between the SMB after and before the $\partial z_s/\partial t$ field adjustment for the simulations $n = 3$ and $n = 4$, respectively. Note: all SMB data is in ice-equivalent.

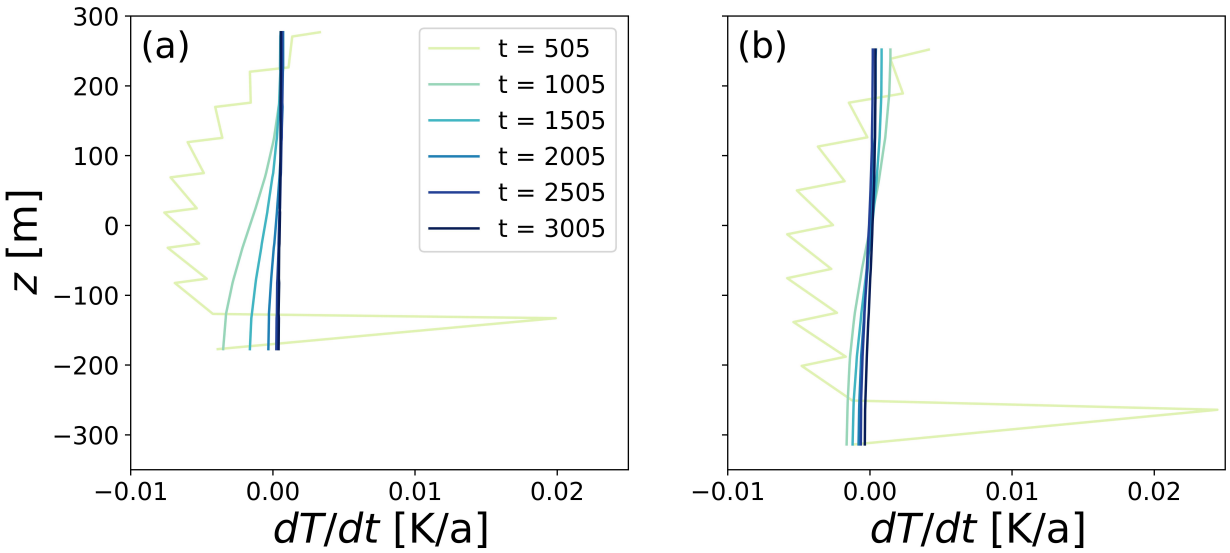

Figure S7. Figures (a) and (b) show the temperature evolution profiles at the horizontal coordinates $(x, y) = (970, 1940)$ and $(x, y) = (960, 1930)$, respectively, during the temperature spin up.

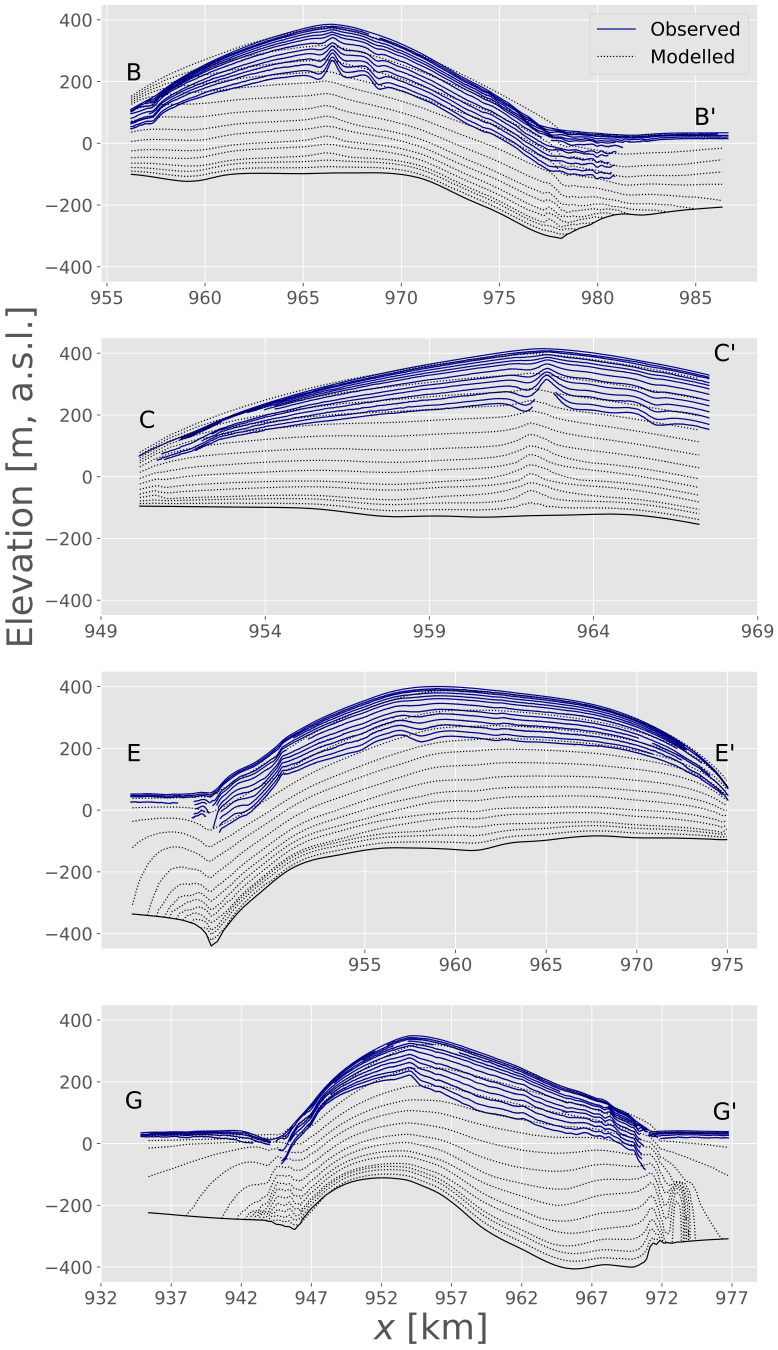

Figure S8. Comparisons between modelled and observed stratigraphy along radar profiles marked in **??** in the vertical domain of the model. Modelled isochrones correspond to the $n = 3$ simulation. The blue solid lines show the observed stratigraphy and the dotted black lines show the modelled stratigraphy.

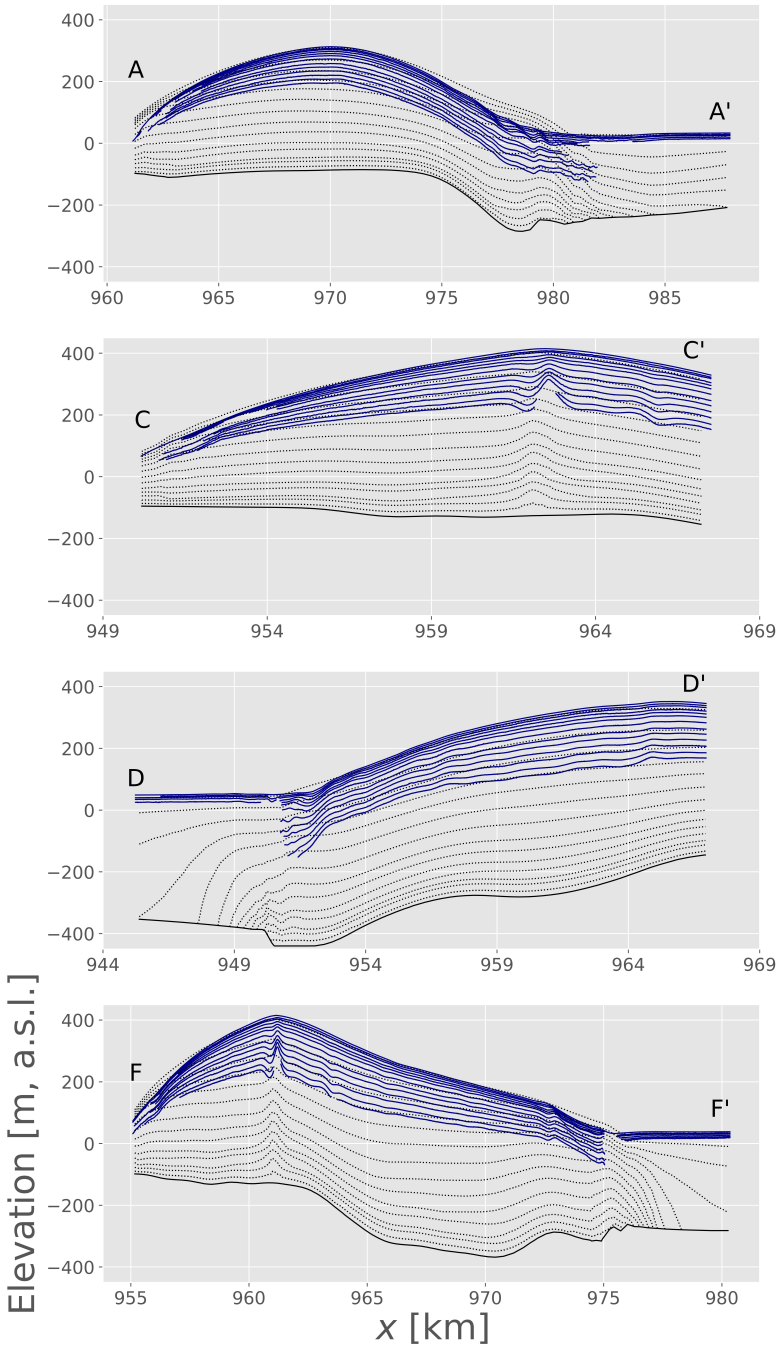

Figure S9. Comparisons between modelled and observed stratigraphy along radar profiles marked in **??** in the vertical domain of the model. Modelled isochrones correspond to the $n = 4$ simulation. The blue solid lines show the observed stratigraphy and the dotted black lines show the modelled stratigraphy.

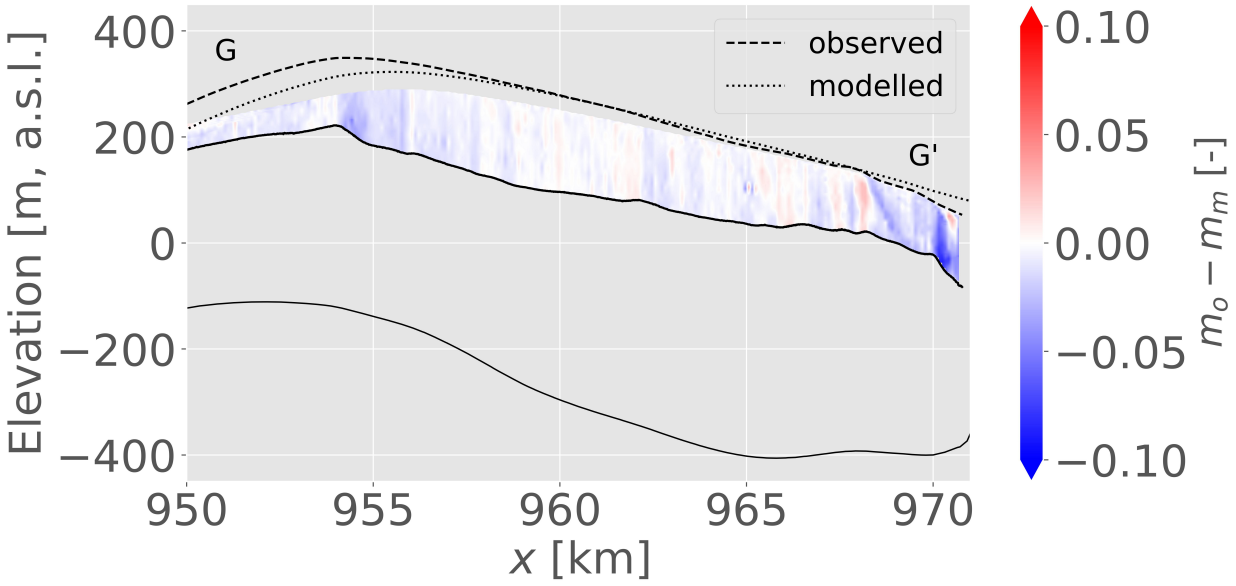

Figure S10. Difference between observed isochrone slope (m_o) and the $n = 3$ modelled isochrone slope (m_m) at locations where data is available for both. The cross-section $G - G'$ corresponds with the radar profile in Fig. 1 in the main article. The dashed lines show the observed ice surface and the dotted lines show the modelled surface. The lower extent of the area of comparison and the lower ice surface are shown with solid black lines.